Article No. jmbi.1998.2329 available online at http://www.idealibrary.com on IDEAL J. Mol. Biol. (1999) 285, 857–873

JMB

Ca^{2+}/Mg^{2+} Exchange in Parvalbumin and other EF-hand Proteins. A Theoretical Study

David Allouche[1], Joseph Parello[2,3] and Yves-Henri Sanejouand[1]*

[1]*Laboratoire de Physique Quantique, UMR 5626 of C.N.R.S., I.R.S.A.M.C. Université Paul Sabatier 118 route de Narbonne 31062 Toulouse Cédex, France*

[2]*UPRES-A CNRS 5074 Faculté de Pharmacie, 15 Av. Ch. Flahault, 34060 Montpellier Cédex 2, France*

[3]*The Burnham Institute, 10901 North Torrey Pines, La Jolla CA 92037, USA*

**Corresponding author*

A remarkable conformational rearrangement occurs upon Ca^{2+}/Mg^{2+} exchange in the C-terminal EF-hand site (labelled site EF or EF-4) of parvalbumin, as initially established by X-ray crystallography. Such a conformational rearrangement is characterised as follows: (i) the co-ordination number decreases from seven oxygen atoms in the Ca-loaded form to six oxygen atoms in the Mg-loaded form, the heptaco-ordination of Ca^{2+} corresponding with a skewed pentagonal bipyramid configuration of the seven oxygen atoms, whereas the hexaco-ordination of Mg^{2+} corresponds with a regular octahedral configuration of the six oxygen atoms; and (ii) Glu101, at the relative position 12 in the EF-hand loop sequence (labelled ''Glu12''), acts as a bidentate ligand in the Ca-loaded form and as a monodentate ligand in the Mg-loaded form. As part of the conformational rearrangement, the χ_1 dihedral angle undergoes a *gauche*(+) to *gauche*(−) transition upon substitution of Ca^{2+} by Mg^{2+}, whereas the χ_2 angle remains practically unchanged and the χ_3 angles in both forms adopt a nearly mirror image relationship. In order to understand the molecular mechanisms underlying such a conformational rearrangement, we undertook a theoretical study using the free energy perturbation (FEP) method, starting from high-resolution crystal structures of the same parvalbumin (pike 4.10 isoform) differing by the substitution of their two cationic sites EF-3 (or CD) and EF-4 (or EF), i.e. the 1pal structure with EF-3(Ca^{2+}) and EF-4(Ca^{2+}), the 4pal structure with EF-3(Ca^{2+}) and EF-4(Mg^{2+}). When Mg^{2+} is ''alchemically'' transformed into Ca^{2+} within the EF-4 site of 4pal, the conformational rearrangement of Glu12 is correctly predicted by the FEP calculation. When Ca^{2+} is transformed into Mg^{2+} within the EF-3 site of 4pal, the FEP calculation predicts the topology of the fully Mg-loaded form for which no crystallographic data is presently available. As expected, Glu62 (at the relative position 12 in EF-3 loop) is predicted to be a monodentate residue within a regular octahedral arrangement of six oxygen atoms around Mg^{2+}. We also investigated the behaviour during Ca^{2+}/Mg^{2+} exchange of two other typical EF-hand proteins, troponin C (TnC) and calmodulin (CaM), for which no three-dimensional structure of their Mg-loaded forms is available so far. It is also predicted that the EF-3 site of TnC and the EF-1 site of CaM have their invariant Glu12 residues switching from the bidentate to the monodentate configuration when Ca^{2+} is substituted by Mg^{2+}, with six oxygen atoms being observed in the co-ordination sphere of the alchemically generated Mg^{2+} cation.

Keywords: calciproteins; EF-hand motif; parvalbumin; free energy perturbation; molecular dynamics

Abbreviations used: FEP, free energy perturbation; CaM, calmodulin; TnC, troponin C; Pa, parvalbumin; MD, molecular dynamics.

E-mail address of the corresponding author: yves@irsamc1.ups-tlse.fr

0022-2836/99/020857–17 $30.00/0

Introduction

The EF-hand proteins are a large family of evolutionarily related proteins with Ca^{2+}/Mg^{2+}-mixed type binding sites, including a variety of subfamilies, such as parvalbumin (Pa), troponin C (TnC), calmodulin (CaM), sarcoplasmic calcium-binding protein, the essential and regulatory light chains of myosin, the S100 and VIS subfamilies (Kawasaki & Kretsinger, 1994). In such proteins, Ca^{2+}/Mg^{2+} exchange appears closely related to physiological processes that involve cell excitation and relaxation, like in muscle contraction (Pechère *et al.*, 1977; Rüegg, 1989). In Pa, two Ca^{2+}-Mg^{2+} sites bind Ca^{2+} with the highest affinity observed so far ($K_{Ca} = 10^9\ M^{-1}$) and Mg^{2+} with moderate affinity ($K_{Mg} = 2.5 \times 10^5\ M^{-1}$), in a competitive way (Cox *et al.*, 1977; Cavé *et al.*, 1979; Haiech *et al.*, 1979; Wnuk *et al.*, 1982). In their initial work demonstrating the binding of Ca^{2+} to parvalbumin, Benzonana *et al.* (1972) reported a lower value of 2.5×10^6 to $2.5 \times 10^7\ M^{-1}$ for both sites. However, their binding measurements were made in the presence of competing Mg^{2+}, and this may explain the lower K_{Ca} value thus inferred. In TnC, a dumbell-shaped protein with two lobes, each containing a pair of EF-hand cation-binding sites, one of the pairs (sites EF-3 and EF-4†) corresponds with Ca^{2+}-Mg^{2+} sites with $K_{Ca} = 2 \times 10^7\ M^{-1}$ and $K_{Mg} = 5 \times 10^3\ M^{-1}$, whereas the remaining sites in the N-terminal lobe are Ca^{2+}-specific with $K_{Ca} = 10^5\ M^{-1}$, as initially determined by Potter & Gergely (1975). A ratio of $K_{Ca}/K_{Mg} = 4 \times 10^3$ is thus inferred for the Ca^{2+}-Mg^{2+} sites of Pa and TnC, although both proteins display large differences in their intrinsic affinity constants for Ca^{2+} and Mg^{2+}, by as much as two orders of magnitude. Such an invariance of the K_{Ca}/K_{Mg} ratio is apparently the rule for most EF-hand proteins (Kawasaki & Kretsinger, 1994). However, in the case of CaM a lower ratio of K_{Ca}/K_{Mg} of ca 2.5×10^2 has been reported for the Ca^{2+}/Mg^{2+} sites EF-1 and EF-2 (Tsai *et al.*, 1987).

In the resting eukaryotic cell, at low intracellular Ca^{2+} concentration, these EF-hand proteins are expected to be Mg^{2+} filled, since intracellular Mg^{2+} concentration is kept rather constantly in the millimolar range (Robertson *et al.*, 1981; Hou *et al.*, 1992). Upon muscle relaxation, as reviewed by Rüegg (1989), parvalbumin may take up the Ca^{2+} bound to TnC and CaM, among other calciproteins, because of its high affinity for Ca^{2+}, while Ca^{2+} may bind first to TnC and CaM because of a slow off-rate of Mg^{2+} from parvalbumin (Breen *et al.*, 1985; White, 1988; Falke *et al.*, 1994), thus eliminating the paradox that parvalbumin with its elevated affinity for Ca^{2+} could preferentially sequester most of the intracellular calcium immediately after a Ca^{2+} transient increase upon cell excitation. As shown by Hou *et al.* (1992), using isolated frog skeletal muscle fibres, Pa facilitates muscle relaxation in the 0-20 °C range due to a subtle balance between the temperature-dependence of the Ca^{2+} and Mg^{2+} dissociation rates from Pa and that of the Ca^{2+} uptake rate by the sarcoplasmic reticulum, in agreement with theoretical simulations indicating that Pa would have its greatest relative effect at low temperatures in skeletal muscle of poikilotherms (Gillis *et al.*, 1982). It is well established that Pa is present in relatively large quantities in the muscles of lower vertebrates, whereas in the higher vertebrates it is only present in relatively small amounts. The presence, however, of Pa in the central nervous system of higher vertebrates (Berchtold *et al.*, 1985; Celio, 1985; Pfyffer *et al.*, 1987; Blümcke *et al.*, 1990; Hartig *et al.*, 1996) raises the question of a more general role of Pa in the control of cell excitation and relaxation.

In their cation competition studies, using the firmly bound trivalent cation Gd^{3+} ($K_a = 2 \times 10^{11}$ M) as an NMR paramagnetic relaxation probe, Cavé *et al.* (1979) showed that the ionic radius plays an essential role in the affinity of Pa for the IIA and IIB divalent cations. A maximum affinity is observed for Ca^{2+} and Cd^{2+}, with closely related ionic radii (0.99 and 0.97 Å, respectively), whereas smaller cations, such as Mg^{2+} (0.65 Å) and Zn^{2+} (0.74 Å) display lower binding constants by three to four orders of magnitude. A larger cation such as Sr^{2+} (1.13 Å) only experiences a decrease in affinity by a factor of 10 compared to Ca^{2+}.

As first demonstrated by Declercq *et al.* (1991) in a study of a set of high-resolution crystal structures of the same parvalbumin (isoform pI 4.10 from pike muscle) with their EF-hand sites occupied by Ca^{2+}, Mn^{2+} or Mg^{2+}, some remarkable, although subtle, changes in the protein conformation are associated with the substitution of Ca^{2+} by other divalent cations with different ionic radii, in one or both of the Pa EF-hand cation-binding sites. This crystallographic study led to the discovery that Glu101 in the EF-4 site (or EF) undergoes a transformation from the *gauche*(+) χ_1 rotamer ($\chi_1 = -75°$) in the Ca-loaded form to the *gauche*(−) χ_1 rotamer ($\chi_1 = +60°$) in the Mg-loaded form, while the χ_2 dihedral angle remains unchanged and the χ_3 dihedral angle adopts a nearly mirror image relationship in both forms. As depicted in Figure 1, it appears that the *gauche*(+)↔*gauche*(−) transformation satisfies a well-defined criterion, i.e. the locus of the cation remains practically invariant within the protein tertiary structure, independent of its occupancy by Ca^{2+} or Mg^{2+}. The simple rotation of the Glu101 side-chain around its C^{α}-C^{β} bond, allows a change in the co-ordination number of the central cation, the glutamyl residue contributing as a bidentate ligand for Ca^{2+} and as a monodentate ligand for Mg^{2+}. In the EF-3 (or CD) site of parvalbumin the homologous glutamyl resi-

† The evolution-based nomenclature proposed by Kawasaki & Kretsinger (1994) for EF-hand sites is adopted here: both four-site EF-hand proteins TnC and CaM correspond to sites EF-1 through EF-4, whereas the two-site EF-hand parvalbumin is labelled with sites EF-3 (initially site CD) and EF-4 (initially site EF).

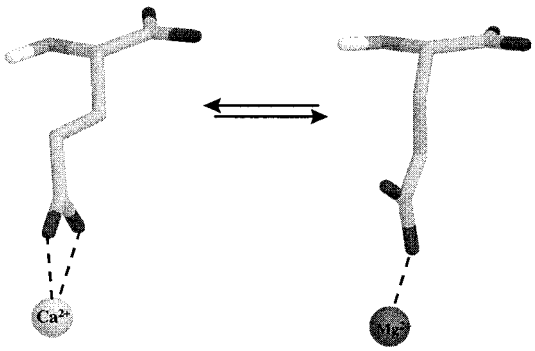

Figure 1. Conformational transition of Glu in relative position 12 of an EF-hand binding site when the co-ordination number of the liganded cation changes by one unit. This transition was described in the case of the EF-4 site of parvalbumin (Declercq *et al.*, 1991).

due Glu62 displays a behaviour similar to that of Glu101 upon Ca^{2+}/Mg^{2+} exchange, as far as the χ_1 angle is concerned, based on NMR evidence (Blancuzzi *et al.*, 1993) and, as suggested by an infra-red study, as far as the bidentate ↔ monodentate switch is concerned (Nara *et al.*, 1994). Both glutamyl residues Glu62 and Glu101 occupy homologous positions in the EF-3 and EF-4 sites of Pa, corresponding with the relative position 12 in the canonical EF-hand loop (Kawasaki & Kretsinger, 1994). Interestingly, Glu12 is highly conserved in all EF-hand loops, Glu being found substituted only by Asp, and in only 8% of all known sequences (Kawasaki & Kretsinger, 1994; Falke *et al.*, 1994). Such a substitution may lead to an inadaptation of the protein to Ca^{2+}/Mg^{2+} exchange, since the bidentate ↔ monodentate transconformation would require a displacement of the cationic locus itself and, thus, of all the other oxygen atoms of the co-ordination sphere.

Whereas the two cation-binding sites of parvalbumin, EF-3 and EF-4, are usually described as displaying indistinguishable affinity constants for Ca^{2+}, if not identical (Kawasaki & Kretsinger, 1994), a detailed kinetic study of whiting Pa using the calcium-dependent fluorescence properties of this Trp-containing parvalbumin (White, 1988) provided evidence that four distinct microscopic equilibrium constants for Ca^{2+} need to be distinguished when the apo-protein is titrated with Ca^{2+} in line with the occurrence of four possible distinct molecular species, i.e. Pa.0.0, Pa.Ca.0, Pa.0.Ca and Pa.Ca.Ca. These four equilibrium constants for Ca^{2+} may differ by as much as five orders of magnitude (lying between $2 \times 10^5\ M^{-1}$ and $1.2 \times 10^{11}\ M^{-1}$) due to very different Ca^{2+} off-rate constants (from 500 to 0.001 s^{-1}) whereas the Ca^{2+} on-rate constants are very similar (in the 1×10^8 to $6 \times 10^8\ M^{-1}\ s^{-1}$ range). Such a study appears to be consistent with a study by Permyakov *et al.* (1980a,b), stating that there are two stoichiometric equilibrium constants for Ca^{2+} binding to whiting parvalbumin, namely, $5 \times 10^8\ M^{-1}$ and $6 \times 10^6\ M^{-1}$ for the first and second Ca^{2+} bound, respectively. These studies with an intrinsic protein chromophore suggest that both cation-binding sites, EF-3 and EF-4, display rather distinct affinities for Ca^{2+}. The observation by Declercq *et al.* (1991) that the EF-3 site (or CD site) was selectively substituted by Ca^{2+} during crystallisation of the Mg-loaded pike 4.10 Pa, in the presence of an excess of Mg^{2+}, also points to the occurrence of two EF-hand sites with distinct affinities for a given divalent cation.

There is evidence that Pa displays a third low-affinity cation-binding site (Declercq *et al.*, 1991, and references therein). In their competition studies with carp 4.25 Pa using Mn^{2+} as an NMR water relaxation paramagnetic probe, Cavé *et al.* (1979) established that the third site displays similar affinities for a variety of divalent cations (Ca^{2+}, Mg^{2+}, Mn^{2+}, Cd^{2+}), independently of their ionic radii, with K_a values in the mM range. Titration of the fully Cd^{2+}-loaded form (component pI 4.25 from carp) by Mn^{2+} as monitored by ^{113}Cd NMR (Cavé *et al.*, 1982) showed that Mn^{2+} binds to the third site at a distance of ca 5 Å from one of the primary sites, as shown by the differential relaxation (line-width) induced on one of both ^{113}Cd resonances in the spectrum, whereas the other ^{113}Cd resonance remains practically unaffected. This led to the conclusion that the third site was a satellite of one of the primary sites (erroneously assigned to be the EF-4 site, although the corresponding ^{113}Cd resonance was the only one to display a pH-sensitive chemical shift), at close distance of the site whereas it lies far apart from the other site (>10 Å). A subsequent ^{113}Cd NMR study of parvalbumin based on the competition of Cd^{2+} by different lanthanides allowed to revise the assignment of both parvalbumin ^{113}Cd resonances (Drakenberg *et al.*, 1985), so that the third site in parvalbumin was to be viewed as an EF-3 satellite. Such a conclusion appeared subsequently fully substantiated by X-ray crystallographic studies of the fully Mn-loaded form of pike pI 4.10 parvalbumin, as well as of mixed forms with the third site occupied with Mg^{2+} or NH_4^+ (Declercq *et al.*, 1991), in agreement with a structural prediction based on a lanthanide ion luminescence study of parvalbumin in solution (Rhee *et al.*, 1981).

As shown by X-ray crystallography with pike 4.10 parvalbumin (Declercq *et al.*, 1991), the third site involves Asp61 (at the relative position 11), as a specific metal-liganding besides other carboxylate-containing residues shared with the primary EF-3 site, in agreement with the initial prediction of Rhee *et al.* (1981) using the Asp61-containing isoform pI 4.25 from carp muscle. In contrast, the crystal structure of a parvalbumin from shark, with Glu61, showed no indication for any electron density compatible with cation binding at the level of Glu61 (Roquet *et al.*, 1992). It is presently established, based on about 30 amino acid sequences, that both phylogenetic lineages α and β of parv-

albumin display Asp and Glu at position 61 (Kawasaki & Kretsinger, 1994), so that a delineation between both lineages based on the third site does not apply, as initially suggested (Cavé *et al.*, 1982). The third site can also accommodate monovalent cations, although with a lower affinity than that observed for divalent cations (Cavé *et al.*, 1979; Declercq *et al.*, 1991). So far there is no real understanding of the role or influence of this third site on the general cation-binding properties of the Asp61-containing parvalbumins in comparison with the Glu61-containing ones, with apparently no third site (see, however, Drakenberg *et al.*, 1985).

In order to understand the molecular basis underlying Ca^{2+}/Mg^{2+} exchange in parvalbumin, we decided to undertake a theoretical analysis of this protein using two high-resolution crystal structures of the Asp61-containing pike 4.10 isoform (Declercq *et al.*, 1991), i.e. the 1pal structure at 1.65 Å resolution (Pa.CaCa.NH_4), with both its high-affinity sites EF-3 and EF-4 occupied by Ca^{2+} and the third site occupied by an ammonium ion, and the 4pal structure at 1.75 Å resolution (Pa.CaMg.Mg), with the EF-3 site occupied by Ca^{2+} and the EF-4 site occupied by Mg^{2+}, whereas the third site is also occupied by Mg^{2+}. For such an analysis, we chose the free energy perturbation (FEP) method (for a recent review, see Kollman, 1993). Besides the fact that this method is able to describe the conformational changes of the protein associated with cation-exchange, it is also able to provide, to some extent, quantitative information on the relative stabilities of the different cation-protein complexes through the calculation of free energy differences. We also tested the possibility that the conformational adaptability of the Glu side-chain at the relative position 12 is also at play during Ca^{2+}/Mg^{2+}-exchange in the Ca^{2+}-Mg^{2+} sites of TnC and CaM. Finally, the calculations involved the case of the sarcoplasmic calcium-binding protein in which Asp lies in the relative position 12, instead of Glu.

Results

Ca^{2+}/Mg^{2+} exchange in the EF-3 site of parvalbumin

Such an alchemical calculation is appealing, since no fully Mg-loaded structure of any EF-hand protein is known so far. As a starting structure we selected the PaCaMg.Mg crystal structure (4pal) which has been determined at 1.75 Å resolution. Note that our model only includes a spherical domain of the protein structure (see Materials and Methods). In our calculation, this domain is centred on the cation in the EF-3 site. Its radius is 15 Å, i.e. all side-chains of the cation-liganding residues are included. Obviously, the PaMgMg.Mg structure obtained as a result of the cation transformation in the EF-3 site during the FEP calculation will not be totally realistic, owing to the fact that a relatively large part of the protein is being held fixed during the calculation.

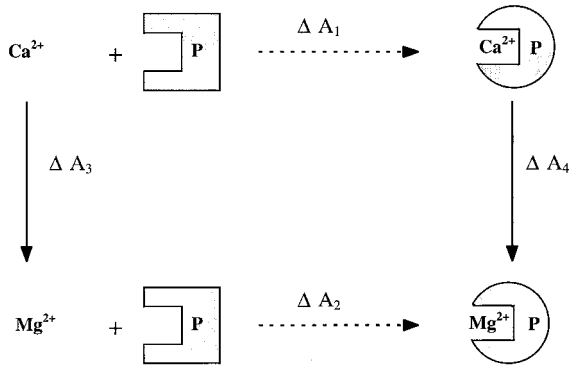

Figure 2. Thermodynamic cycle used to compute the relative free energy difference ($\Delta\Delta A$) associated to Mg^{2+} *versus* Ca^{2+} binding, by parvalbumin and other EF-hand proteins. In practice, $\Delta\Delta A = \Delta A_2 - \Delta A_1$ is computed as $\Delta\Delta A = \Delta A_4 - \Delta A_3$, through the alchemical transformation of $Ca^{2+} \rightarrow Mg^{2+}$, in water on the one hand (ΔA_3), and in the studied protein EF-hand site, on the other hand (ΔA_4).

In Figure 2, the thermodynamical cycle associated with Ca^{2+}/Mg^{2+} exchange in parvalbumin is shown. Here, P represents the parvalbumin in different conformational states. Note that within such a scheme, no knowledge of the conformational state of parvalbumin with its EF-3 site devoid of any cation is required, since in the calculation of the ΔA_3 free energy difference, the energy terms associated with the protein cancel out. Moreover, as recalled in Material and Methods, with the parameter set used in the present study (Åqvist, 1990), cation free energy differences in water are very well reproduced, that is, the calculated ΔA_3 (−77.0(±0.4) kcal/mol) is found to lie close to experimental values, namely −79.0(±1.3) kcal/mol (Gomer & Tryson, 1977; Marcus, 1994).

The step-by-step ($\Delta\lambda = 0.1$) alchemical transformation of PaCaMg.Mg (4pal) into PaMgMg.Mg is illustrated in Figure 3 with respect to some critical geometrical features of the EF-3 site upon Ca^{2+}/Mg^{2+} exchange by plotting: (i) the variation of time-averaged cation-oxygen distances as a function of the transformation parameter λ; and (ii) the variation of the three torsional angles χ_1 through χ_3 of Glu62. When $\lambda = 0.05$, seven oxygen atoms are co-ordinating the Ca^{2+}-like cation at a mean distance of 2.3 Å. This latter value happens to be significantly lower than the corresponding mean distance in the crystal structure, namely, 2.4 Å (Declercq *et al.*, 1991). Moreover, an eighth oxygen atom, the $O^{\varepsilon 2}$ of Glu59, lies in the calculated structure at a distance, 2.7 Å, significantly shorter than in the crystal structure, namely, 3.5 Å. This certainly reflects the inaccuracies of the force field used to describe cation-oxygen interactions (see Discussion). A topology with seven oxygen atoms in the co-ordination shell of the cation,

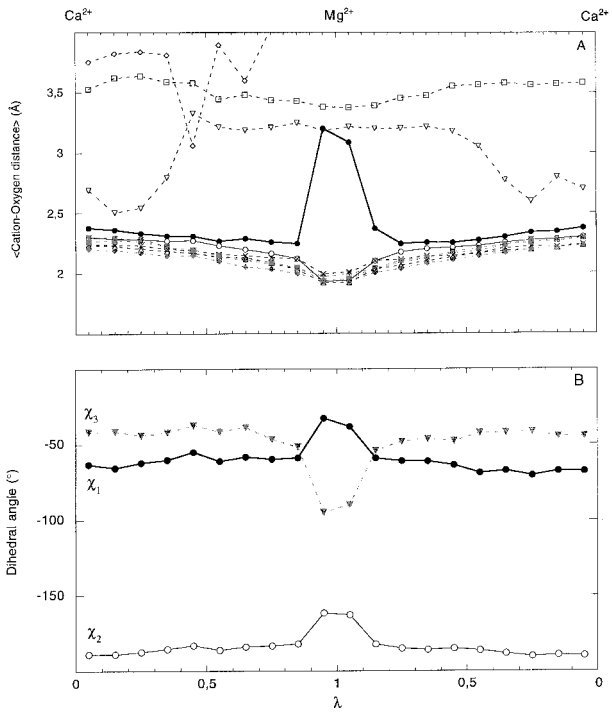

Figure 3. $Ca^{2+} \rightarrow Mg^{2+}$ transformation within the EF-3 site of parvalbumin. (a) Average cation-oxygen distances. Diamonds, Asp51 carboxylate oxygen atoms; squares, Asp53 carboxylate oxygen atoms; triangle, Ser55 hydroxyl oxygen; cross, Phe57 carbonyl oxygen; reverse triangles, Glu59 carboxylate oxygen atoms; circles, Glu62 carboxylate oxygen atoms. (b) Average values of the three torsional angles of the Glu62 side-chain, for each value of λ ($\lambda = 0$ corresponds to the Ca state of the cation, while $\lambda = 1$ corresponds to its Mg state). Glu62 is in relative position 12 of the EF-hand motif.

which is expected in the case of a Ca^{2+}-like atom, is clearly restored when λ becomes larger than 0.35, and this topology is kept when λ increases up to $\lambda = 0.85$. A general decrease in the cation-oxygen distances is observed as the λ value increases, which is correlated with the ionic radius decrease of the simulated cation (see Materials and Methods), in agreement with X-ray crystallographic studies of parvalbumins substituted by divalent cations differing in their ionic radii, namely, Ca^{2+}, Cd^{2+}, Mn^{2+} and Mg^{2+} (Declercq *et al.*, 1991; Swain *et al.*, 1989). During the last step of the simulation ($\lambda = 0.95$), the $O^{\varepsilon 1}$ oxygen of Glu62 leaves the co-ordination sphere and becomes an outer shell atom at a distance greater than 3 Å from the central cation, Mg^{2+}-like, whereas the $O^{\varepsilon 2}$ oxygen of Glu62 comes significantly closer to the cation. This corresponds to the transformation of Glu62 from a rather symmetrical bidentate ligand to a monodentate one. At this point, the co-ordination shell of the cation corresponds with a strict hexaco-ordination, in agreement with crystallographic data on the EF-4 binding site of the PaCaMg.Mg structure, as well as with numerous structural data on solvated Mg^{2+} (Ohtaki & Radnai, 1993). However, mean Mg^{2+}-oxygen distances, namely, 1.9 Å, are significantly shorter than experimentally observed ones, namely, 2.1 Å, in the EF-4 site of 4pal, and 2.00-2.15 Å for Mg^{2+}-water oxygen distances (Ohtaki & Radnai, 1993). This latter fact certainly also reflects the inaccuracies of the force field used. Note that rather symmetrical results are observed in the reverse simulation, that is, when λ is decreasing from $\lambda = 0.95$ to the initial $\lambda = 0.05$ value. This means that the results found at each λ value do not depend too much on the way the initial conditions of each simulation are determined. It also means that the time span of the simulations performed at each λ value is large enough, so that it allows for a reasonable equilibration of the system between each $\Delta\lambda$.

Since we observed that Glu62 undergoes the most dramatic change during the $Ca^{2+} \rightarrow Mg^{2+}$ transformation, we also plotted the variations of the three torsional angles χ_1 through χ_3 of Glu62 as a function of λ (Figure 3(b)). All three angles remain practically unchanged for λ values in the range 0.05-0.85. A marked variation is observed when $\lambda = 0.95$, as Glu62 becomes a monodentate ligand of the central cation, χ_1 varying from nearly -60° to -30°, χ_2 from nearly -190° to -160° and χ_3 from nearly -40° to -90°. Although our theoretical approach clearly predicts that Glu62, in the EF-3 site, undergoes a transformation from a bidentate to a monodentate ligand, the latter results markedly differ from what was expected from the comparison of the crystal structures PaCaCa.NH_4 (1pal), or PaCaCa.Mg (3pal), with PaCaMg.Mg (4pal). It was found that substitution of Ca^{2+} by Mg^{2+} in the EF-4 site corresponds with a large variation of χ_1, a nearly zero variation of χ_2, and a significant variation of χ_3. As a matter of fact, the χ_1-χ_3 values of Glu62 observed during the $\lambda = 0.95$ simulation are very close, within 10°, to those of Glu101, when the EF-4 site is occupied by Mn^{2+} (Declercq *et al.*, 1991).

As described in Materials and Methods, each simulation at a given λ value is performed with a 5 ps equilibration period followed by a 10 ps trajectory. Thus, the question of whether the system is fully relaxed after 15 ps at $\lambda = 0.95$ has to be addressed, as well as whether the behaviour of the system at this λ value is different from its behavior at $\lambda = 1.0$, i.e. when the central cation in the EF-3 site is a ''pure'' Mg^{2+}. Thus, a 100 ps molecular dynamics (MD) simulation was performed, with $\lambda = 1.0$, starting from the point reached at the end of the $\lambda = 0.95$ calculation. As shown in Figure 4, a remarkable feature is observed during this trajectory, as far as the Glu62 torsional angles are concerned. Whereas the χ_2 angle remains stabilised at a mean value of -170° all along the trajectory (data not shown), this is not the case for both χ_1 and χ_3 angles. In the first half of the trajectory, χ_1 and χ_3 transition spikes are observed, both angle variations being strongly correlated. In contrast, in the second half of the 100 ps trajectory, relatively

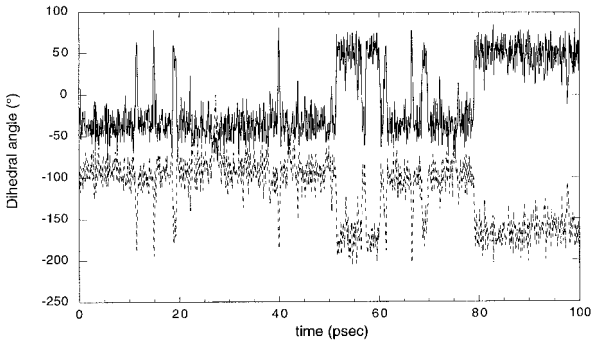

Figure 4. Dynamical behaviour of the χ_1 (continuous line) and χ_3 (broken line) torsional angles of the Glu62 side-chain, during a 100 ps time span starting at the end of the $Ca^{2+} \rightarrow Mg^{2+}$ transformation within the EF-3 site of parvalbumin. The χ_2 angle remains rather constant around a $-170°$ value (data not shown).

long-lasting variations of χ_1 and χ_3 are observed, χ_1 jumping from nearly $-40°$ to $+50°$, and χ_3 from nearly $-90°$ to $-180°$. As found when a longer trajectory is considered (100 ps more, data not shown), Glu62 is in equilibrium between two states, one observed when $\lambda = 0.95$ and in the most part of the 50 first ps of the trajectory performed at $\lambda = 1.0$, and the other one observed nearly half of the time during the remaining 50 ps of the trajectory performed at $\lambda = 1.0$ (see Figure 4), as well as later on (data not shown). Interestingly, the latter conformational state is very close to the one observed with Glu101, in the Mg-loaded form of the EF-4 site (see Table 1). Since the system we studied is restricted to a sphere around the EF-3 site, and since it is likely that an unrestricted system would have more possibilities to relax, our results strongly suggest that upon Ca^{2+}/Mg^{2+}-exchange the EF-3 binding site undergoes a conformational rearrangement very similar to the one experimentally observed in the EF-4 site. Geometrical features of the EF-3 site occupied by Mg^{2+}, as inferred from one snapshot picked near the end of the 100 ps trajectory performed with $\lambda = 1.0$ (Figure 4), are shown in Figure 5. It underlines the fact that $\chi_1 = +50°$, $\chi_2 = -170°$ and $\chi_3 = -180°$ in the Glu62 side-chain correspond with a quite regular oxygen octahedron around the central cation, in agreement with the known features of the EF-4 site, when it is occupied by Mg^{2+}.

The possibility that the Glu12 side-chain happens to be highly flexible within the EF-hand sites of parvalbumin has also to be considered. To do so, another 100 ps MD simulation was carried out starting from the crystal structure PaCaMg.Mg, with $\lambda = 0.0$, i.e. in the case of EF-3 loaded with a pure calcium. A single conformational state is observed for Glu62 over the entire trajectory (data not shown). It is similar to the state observed at $\lambda = 0.05$ during the FEP calculation (see Figure 3). Thus, the occurrence of a conformational equilibrium for the Glu62 side-chain seems to be unlikely in the Ca-loaded form.

The free energy calculations carried out with both systems described in the legend to Figure 2, the cation in water on the one hand, and the protein-bound cation on the other hand, allow for the calculation of the corresponding free energy difference. As shown in Table 2, a value of $\Delta\Delta A = \Delta A_4 - \Delta A_3 = 4.4(\pm 0.5)$ kcal/mol was obtained, which corresponds with a ratio of Ca^{2+} and Mg^{2+} affinity constants of roughly 10^3 at room temperature, in good agreement with experimental data (see Introduction). The relevance of such a result will be discussed below. It suggests that the model and the potential energy function used in the present study are able to lead, in spite of different approximations, to a quite good description of the main energetical features of an EF-hand binding site.

Mg^{2+}/Ca^{2+} exchange in the EF-4 site of parvalbumin

The PaCaMg.Mg crystal structure (4pal) was also taken as a starting point to investigate Mg^{2+}/Ca^{2+} exchange within the EF-4 site. Such an additional FEP calculation is intended to be a test of the validity of the approach used in order to obtain the above results, on the EF-3 site of parvalbumin, as well as on other EF-hand sites (see below), since the structure to be reached at the end of the calculation, PaCaCa.Mg, is already known by X-ray crystallography (3pal).

Table 1. Dihedral angles (in degrees) of the glutamate side-chain at the relative position 12 of the EF-hand motifs of parvalbumin

EF-hand motif	Cation	χ_1	χ_2	χ_3
EF-3: crystal structures[a]	Ca^{2+}	−78, −67, −72	175,169,176	−12, −9, −24
EF-4: crystal structures[b]	Ca^{2+}	−78, −72	−179, −177	−31, −37
EF-4: crystal structure[c]	Mg^{2+}	62	−172	−167
EF-3: simulated structure	Mg^{2+}	50	−170	−180

Comparison between experimental (Declercq *et al.*, 1991) and theoretical data. The simulated structure corresponds with the conformational state achieved within the 80-100 ps region of the MD trajectory (see Figure 4).

[a] Dihedral angles of Glu62 in crystallographic structures 1pal, 3pal and 4pal, respectively.

[b] Dihedral angles of Glu101 in crystallographic structures 1pal and 3pal, respectively.

[c] Dihedral angles of Glu101 in the crystallographic structure 4pal.

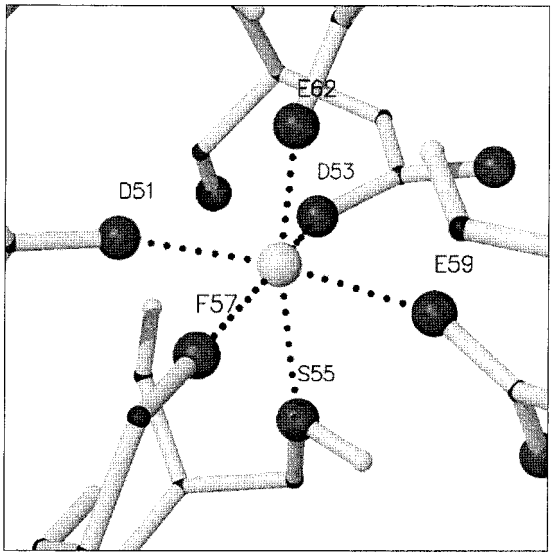

Figure 5. Predicted geometry of the EF-3 site of parvalbumin, when it is occupied by Mg^{2+}. Oxygen atoms and the magnesium atom are represented as large spheres, grey and white ones, respectively. A dotted line means that the corresponding cation-oxygen distance is smaller than 2.0 Å. The geometry displayed corresponds with a snapshot along the MD trajectory within the 80-100 ps region (see Figure 4) so that the monodentate Glu62 displays the χ_1 *gauche*(−) rotamer. This Figure was drawn with the Molscript program (Kraulis, 1991).

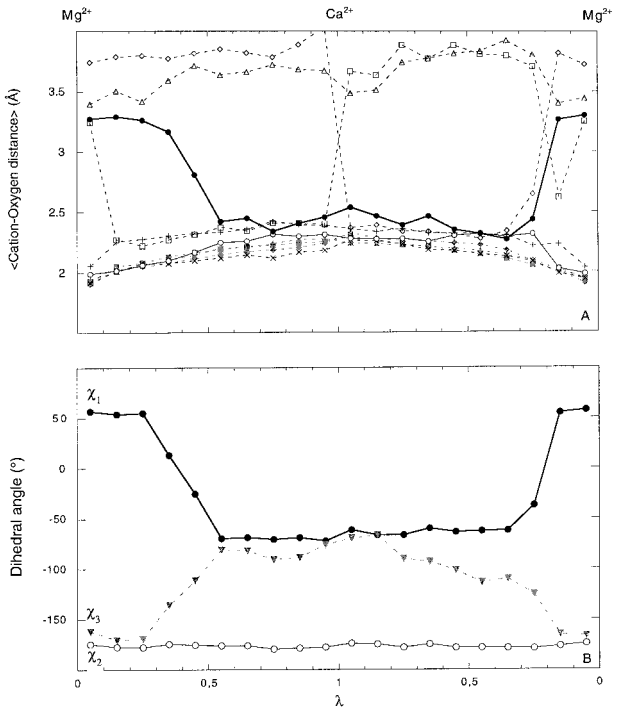

Figure 6. $Mg^{2+} \rightarrow Ca^{2+}$ transformation within the EF-4 site of parvalbumin. (a) Average cation-oxygen distances. Diamonds, Asp90 carboxylate oxygen atoms; squares, Asp92 carboxylate oxygen atoms; triangles, Asp94 carboxylate oxygen atoms; cross, Met96 carbonyl oxygen; circles, Glu101 carboxylate oxygen atoms; plus, water 246 hydroxyl oxygen. (b) Average values of the three torsional angles of the Glu101 side-chain, for each value of λ ($\lambda = 0$ corresponds with the Mg state of the cation, while $\lambda = 1$ corresponds with its Ca state). Glu101 is in relative position 12 of the EF-hand motif.

As indicated in Figure 6(a), when $\lambda = 0.05$ (Mg-state) the cation is hexaco-ordinated, its ligands being Asp90, Asp92, Asp94, Met96 (main-chain C = O), a water molecule along the −X direction, and Glu101 (monodentate) along the −Z direction, at the relative position 12 of this EF-hand motif. During the $Mg^{2+} \rightarrow Ca^{2+}$ transformation, as soon as $\lambda = 0.15$, Asp92 becomes a bidentate ligand. This is probably not a meaningful result, since in all known crystal structures of Ca-loaded parvalbumins, Asp92 behaves as a monodentate ligand. However, both oxygen atoms of Asp92 remain close to the central cation up to $\lambda = 0.95$, the Ca-state. At $\lambda = 0.55$, Glu101 becomes a bidentate ligand, so that the cation co-ordination number rises to eight.

On the other hand, the backward $Ca^{2+} \rightarrow Mg^{2+}$ transformation is first characterised by an exchange of liganding oxygen atoms which occurs at $\lambda = 0.95$. Whereas Asp90 becomes bidentate, Asp92 switches simultaneously from the bidentate to the monodentate configuration. Thus, the cation co-ordination number remains equal to eight, but the nature of the liganding atoms differ from what it is at the end of the $Mg^{2+} \rightarrow Ca^{2+}$ transformation. At $\lambda < 0.25$, both Asp90 and Glu101 residues switch from the bidentate to the monodentate configuration, so that the cation becomes hexaco-ordinated for λ values close to zero, when the system is in a Mg-state, in agreement with experimental data. Note that Asp94, in relative position 5, behaves as a monodentate ligand all along the ''round-trip'' $Mg^{2+} \rightarrow Ca^{2+} \rightarrow Mg^{2+}$ FEP calculation. Moreover, as expected, all cation-oxygen distances within the co-ordination sphere progressively increase during the $Mg^{2+} \rightarrow Ca^{2+}$ transformation, from a mean value of 1.9 Å, up to a mean value of 2.3 Å. As observed during our previous calculation, these distances are slightly shorter than the experimentally determined ones. The instability of the configuration of the eight oxygen atoms around Ca^{2+}, exhibited in the $\lambda = 0.95$ simulations is not presently understood, but it is likely that it is

Table 2. Relative free energy difference ($\Delta\Delta A$), in kcal/mol, associated to the $Ca^{2+} \rightarrow Mg^{2+}$ alchemical transformation in water and in parvalbumin EF-hand sites, starting from three different crystallographic structures

Structure	EF-3 site	EF-4 site
PaCaMg.Mg (4pal)	4.4 ± 0.5	-1.5 ± 2.1
PaCaCa.Mg (3pal)	2.9 ± 0.0	-0.5 ± 0.0
PaCaCa.NH_4 (1pal)	5.1 ± 0.3	6.6 ± 1.9

The hysteresis measured at the end of the $Ca^{2+} \rightarrow Mg^{2+} \rightarrow Ca^{2+}$ transformation is given as an estimation of the accuracy of our calculations. With our model and parameter set, the free energy difference between the two cations in water is nearly −77.7 kcal/mol.

also a consequence of the inaccuracies of the potential energy function used here, since it occurs in the context of an incorrect prediction, namely, that there are more than seven oxygen atoms in the coordination shell of Ca^{2+}. Note, however, that octaco-ordination of Ca^{2+} has often been observed, in particular during MD simulations of this cation in a water environment (Allouche, 1997; Periole *et al.*, 1997; 1998, and references therein), but also in many crystal structures of small molecules (Kaufman-Katz *et al.*, 1996).

It is clear that the pattern shown in Figure 6(a) is less symmetrical than the corresponding pattern shown in Figure 3(a), i.e. the one associated with Ca^{2+}/Mg^{2+}-exchange within the EF-3 site. However, the conformational behaviour of the Glu101 side-chain is much more symmetrical, as judged by the variation of the torsional angles χ_1-χ_3 all along the round-trip transformation (see Figure 6(b)), than in the previous case (Figure 3(b)). The χ_2 value remains almost constant all along the transformations, at a -180° value which corresponds to a *trans* rotamer about the C^β-C^γ bond. In the initial Mg-loaded form, $\chi_1 = +50^\circ$ corresponds to the *gauche*(−) rotamer about the C^α-C^β bond, whereas at the end of the $Mg^{2+} \rightarrow Ca^{2+}$ transformation, $\chi_1 = -60^\circ$ corresponds to the *gauche*(+) rotamer, χ_3 switching simultaneously from -170° to -60°, in nearly perfect agreement with what is found in the crystal structure of the fully Ca-loaded form PaCaCa.Mg (3pal), as well as in PaCaCa.NH_4 (1pal; see Table 1) in spite of the fact that the filling of the third site is different in this latter structure.

Finally, though the structural features observed during the FEP calculation itself with EF-4 are closer to experimental data than in the calculation with EF-3, the free energy difference value obtained seems at variance with the experimental result (see Table 2), since the affinity of the EF-4 site for Mg^{2+} is found to be greater, or at best equal, to its affinity for Ca^{2+}. This is a rather paradoxical result, since the value obtained in the case of the EF-3 site was found to be a quite reasonable one in comparison with the experimental data. However, the possibility that this result is also meaningful may have to be taken seriously, since it is consistent with the fact that PaCaMg.Mg was crystallised as a unique form (Declercq *et al.*, 1991). Indeed, if the EF-4 site was found occupied by Mg^{2+} in all crystal cells of this form, the EF-3 site being occupied by Ca^{2+}, this means that the ratio of the affinity constants for Ca^{2+} and Mg^{2+} is larger in the case of the EF-3 site than in the case of the EF-4 site, at least in the conditions used to crystallise the PaCaMg.Mg form, i.e. at low Ca^{2+} (impurity level) and very high Mg^{2+} concentrations (magnesium sulfate was used as the precipitating agent). One possibility is that such a distinction between the binding properties of the two parvalbumin EF-hand sites occurs when the so-called ''third site'' of parvalbumin (Declercq *et al.*, 1991) is occupied by Mg^{2+} instead of a monovalent cation (ammonium) in the 1pal structure. In order to test this hypothesis, other FEP calculations were performed, starting from the fully Ca-loaded forms PaCaCa.Mg (3pal) and PaCaCa.NH_4 (1pal), in which the third site is occupied by Mg^{2+} and NH_4^+, respectively. As shown in Table 2, the $\Delta\Delta A$ values obtained at the end of $Ca^{2+} \rightarrow Mg^{2+}$ transformations in the EF-3 site of PaCaMg.Mg, PaCaCa.Mg or PaCaCa.NH_4 are of similar magnitude, ranging between 2.9 and 5.1 kcal/mol. When such a transformation is performed within the EF-4 site of PaCaCa.NH_4, the $\Delta\Delta A$ value obtained is also a large one, namely, 6.6 kcal/mol. As a matter of fact, in the case of this latter structure (1pal), both EF-hand sites of parvalbumin display similar relative binding properties with respect to Ca^{2+} and Mg^{2+}, in agreement with standard experimental data, as well as with the hypothesis that the binding properties of the EF-4 site of parvalbumin are not the usual ones when the third site is occupied by Mg^{2+}, like in 3pal or 4pal.

As far as the dynamical behaviour of Glu in relative position 12 upon Ca^{2+}/Mg^{2+}-exchange is concerned, in the two FEP calculations performed with the EF-3 site, starting from the Ca-loaded forms 1pal and 3pal, no clear dihedral transition is observed, even when a 100 ps trajectory is performed at $\lambda = 1.0$. In the calculations with the EF-4 site, dihedral transitions are observed in the case of 1pal, when 100 ps more at $\lambda = 1.0$ are performed, but they are significantly different from the experimentally known one (χ_2 being involved in the transition, for instance). Nevertheless, all calculations correctly predict an hexaco-ordination for Mg^{2+}, Glu in relative position 12 becoming monodentate upon Ca^{2+}/Mg^{2+}-exchange.

Mg^{2+}/Ca^{2+} exchange in other EF-hand proteins

As shown in Figure 7, a symmetrical round-trip pattern is observed in the case of the Ca^{2+}/Mg^{2+}

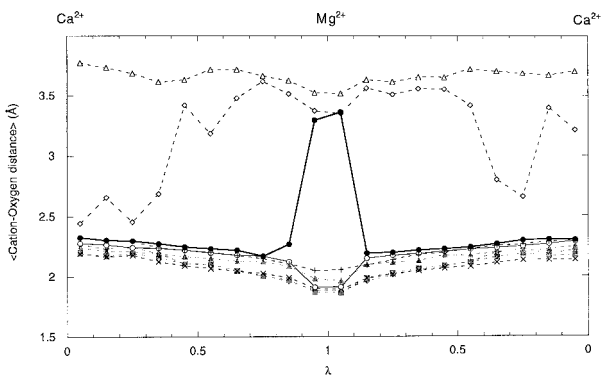

Figure 7. $Ca^{2+} \rightarrow Mg^{2+}$ transformation within the EF-3 site of troponin C, average cation-oxygen distances, for each value of λ ($\lambda = 0$ corresponds with the Ca state of the cation, while $\lambda = 1$ corresponds with its Mg state). Diamonds, Asp106 carboxylate oxygen atoms; squares, Asn108 carboxylate oxygen; triangles, Asp110 carboxylate oxygen atoms; cross, Phe112 carbonyl oxygen; circles, Glu117 carboxylate oxygen atoms; plus, water176 hydroxyl oxygen.

exchange in the EF-3 site of troponin C. This pattern is rather similar to the one calculated for the parvalbumin EF-3 site (see Figure 3(a)). The Glu117 of troponin C, which is homologous to Glu62 of parvalbumin, undergoes a transition from a bidentate (Ca-loaded site) to a monodentate configuration (Mg-loaded site). At the end of the $Ca^{2+} \rightarrow Mg^{2+}$ transformation, the conformational state of Glu117 is closely related to the state obtained at the same point, in the case of parvalbumin Glu62 (see Figure 3(b)). Noteworthy, no *gauche*(+) → *gauche*(−) transition is observed for χ_1 (data not shown). Very similar results are obtained when the Ca^{2+}-Mg^{2+} EF-1 site of calmodulin (Tsai *et al.*, 1987) is studied, Glu31 (in relative position 12 of EF-1) undergoing the bidentate to monodentate transition (data not shown). Finally, since in all our calculations the crucial role of Glu in relative position 12 on Ca^{2+}/Mg^{2+} exchange is underlined, a FEP calculation was performed in the case of the EF-1 site of the sarcoplasmic calcium-binding protein (Vijay-Kumar & Cook, 1992) in which an Asp lies in relative position 12 (Asp27). In this case, a hexaco-ordination of Mg^{2+} is also predicted but Asp12 remains bidentate all along Ca^{2+}/Mg^{2+}-exchange, while Asp3 (Asp18), along the *Y* axis, switches from the bidentate to the monodentate configuration (data not shown).

Discussion

The alchemical substitution of Mg^{2+} by Ca^{2+} in the EF-4 site of Pa allowed us to test the validity of our theoretical predictions in the light of both known states of the EF-4 site, Ca^{2+} or Mg^{2+}-loaded, in the high-resolution crystal structures 1pal and 4pal, respectively (Declercq *et al.*, 1991). As shown in Figure 6(a), the most striking trend is the progressive adaptation upon λ variation of the oxygen-cation distances for all co-ordinating atoms to the evolution of the ionic radius (as simulated by the λ variation), with the exception of the carboxylate oxygen atoms of Glu101. Indeed, the carboxylate $O^{\varepsilon 2}$ atom of Glu101 enters (Ca^{2+} binding) or leaves (Mg^{2+} binding) the co-ordination sphere of the cation during the alchemical transformation. The $O^{\varepsilon 1}$ atom, the other carboxylate oxygen, follows the adaptive trend of the other oxygen atoms and remains constantly part of the co-ordination sphere of the central cation. The fact that Glu101 switches between a monodentate ligand (Mg^{2+} binding) and a bidentate ligand state (Ca^{2+} binding) in the parvalbumin EF-4 site during the FEP calculation with 4pal apparently validates our approach. Furthermore, as shown in Figure 6(b), the rearrangement observed at the level of Glu101 is characterised by a variation of both dihedral angles χ_1 and χ_3, whereas χ_2 remains constant, in agreement with X-ray crystallographic data. Thus, taken together, the results presented in Figure 6 are satisfactorily mimicking the structural features observed experimentally, the conformational rearrangement of the Glu101 side-chain upon Ca^{2+}/Mg^{2+}-exchange being remarkably well predicted. These results justify our attempt to use the same approach in the case of the parvalbumin EF-3 site for which only the Ca^{2+}-bound state is known, as far as crystallographic evidences are concerned, as well as in the case of other EF-hand proteins (TnC and CaM) for which no tertiary structure with bound Mg^{2+} is known so far.

At present, a tertiary structure of parvalbumin with both its primary sites, EF-3 and EF-4, occupied by Mg^{2+} is not available. As shown in Figure 5, starting from the 4pal crystal structure, or Pa.CaMg.Mg, our approach leads to a geometry of the Mg^{2+}-loaded EF-3 site, in the structurally unknown Pa.MgMg.Mg form. Since the calculations were only carried out with a protein subdomain and not with the whole protein molecule (see Materials and Methods), the fully Mg^{2+}-loaded form thus generated is not to be considered as a totally realistic tertiary structure of the novel Pa.MgMg.Mg form. However, we consider the geometrical features of the EF-3 site itself to be structurally accurate. Indeed, the predicted structure fully satisfies the co-ordination requirements of Mg^{2+} by an EF-hand motif, the hexaco-ordination being sharply defined with a regular octahedral arrangement of the liganding oxygen atoms around the central cation (see Figure 5). Moreover, as expected, Glu62, which is homologous to Glu101 in the EF-4 site, acts as a monodentate ligand.

It is interesting to note that Strynadka & James (1989) speculated that the co-ordination geometry of the HLH sites in the EF hand proteins with an invariant glutamyl residue at the relative position 12 in the loop are designed to accommodate, separately, both Ca^{2+} and Mg^{2+}: (i) in order to adapt the site so that it would bind Mg^{2+}, subtle changes in the torsional angles χ_2 and χ_3 would rotate the Glu12 carboxylate group so that its plane would be approximately perpendicular to the equatorial plane: in this configuration only one of the Glu12 carboxylate would still be on the equatorial plane (as in Ca^{2+} co-ordination) and co-ordinating to the metal ion along the $-Z$-axis, allowing the other five co-ordinating ligands to cluster more closely around a smaller Mg^{2+} with the appropriate octahedral co-ordination; and (ii) subtle adaptations with rotations of ca 30° about χ_1 in the residues at positions *X*, *Y* and *Z* could finally adapt to Mg^{2+} co-ordination. As experimentally determined in the case of parvalbumin (Declercq *et al.*, 1991) with its EF-4 site occupied by Ca^{2+} and Mg^{2+} (1pal and 4pal crystal forms, respectively): (i) the Mg^{2+}-substituted form adopts a strictly octahedral co-ordination with Glu12, i.e. Glu101, acting as a monodendate, in agreement with the predictions by Strynadka & James (1989), whereas Ca^{2+} in the EF-4 site is heptaco-ordinated with Glu101 acting as a bidentate ligand within a skewed pentagonal bipyramid; (ii) however, the main variation in the torsional angles of Glu12 based on the crystallo-

graphic data resides in χ_1 with ca 120° variation (barrier dependent transconformation) between both forms, Ca^{2+} and Mg^{2+} substituted, whereas χ_2 remains practically unaffected and χ_3 undergoes a variation of ca 40° in order to optimise the octahedral geometry around Mg^{2+}, in contrast with the predictions by Strynadka & James (1989). Such a conformational rearrangement upon Ca^{2+}/Mg^{2+}-exchange at the level of the EF-hand site can be viewed as a ''crankshaft'' motion with a C^{α}-C^{β} axis (passing through one of the co-ordinating O^{ε}) remaining practically invariant, whereas the cranked segment undergoes ca 120° rotation around the axis; (iii) finally, the residues along *X*, *Y* and *Z* show an adaptation of their χ_1 torsional angles with no crossing of a barrier (variations within 30°). Apparently, a larger conformational repertoire is to be considered at the level of Glu12 if one considers the rearrangement of the glutamyl side-chain upon substitution of Ca^{2+} by Mn^{2+} (the latter has an ionic radius intermediate between those of Ca^{2+} and Mg^{2+}). In the EF-4 site substituted by Mn^{2+} (crystal structure 2pal; Declercq *et al.*, 1991), Glu12 has all its three torsional angles χ_1, χ_2 and χ_3 affected in comparison with the Ca^{2+}-filled form; similarly, the EF-3 site substituted by Mn^{2+} (in the full Mn^{2+}-loaded form 2pal), has its three Glu12 torsional angles χ_1, χ_2 and χ_3 affected. Apparently, subtle structural differences in the cation size as well as in the protein tertiary structure could orient differently the rearrangement of the Glu12 side-chain. Our simulation of Mg^{2+}-co-ordination in the EF-3 site of parvalbumin suggests that all torsional angles χ_1, χ_2 and χ_3 could be involved during Ca^{2+}/Mg^{2+} exchange, without specifically affecting χ_1 which would then remain as a *gauche*(+) rotamer, although skewed. However, upon prolongation of the MD trajectory after alchemical transformation of Ca^{2+} by Mg^{2+} in the parvalbumin EF-3 site (Figure 4), an interconversion between both χ_1 *gauche*(+) and *gauche*(−) rotamers occurs as sharp and complementary transitions of both χ_1 and χ_3 torsional angles, whereas the χ_2 angle remains practically constant, in agreement with the crankshaft-type motion described above.

We note that the Mg-oxygen distances in the simulated EF-3 site are slightly shorter than the experimental mean value observed in the case of the EF-4 site substituted by Mg^{2+} (4pal crystal structure), and this is to be due, as stated above, to some inaccuracies of the potential used to describe protein-cation interactions. A point to be considered more critically is the conformational rearrangement undergone by the side-chain of Glu62 upon substitution of Ca^{2+} by Mg^{2+} in the EF-3 site. In contrast with the side-chain of Glu101 in the EF-4 site, Glu62 displays a variation of all its χ dihedral angles in order to adapt its geometry to the co-ordination of Mg^{2+}, as shown in Figure 3(b). Whereas the side-chain adopts the *gauche*(+) conformation with $\chi_1 = -60°$ in the starting 4pal form, the end of the $Ca^{2+} \rightarrow Mg^{2+}$ transformation is characterised by $\chi_1 = -40°$ which corresponds with a skewed *gauche*(+) rotamer with, therefore, no switch to the *gauche*(−) rotamer (as is the case of Glu101). However, if the MD trajectory is pursued for 100 ps (Figure 4), the dihedral angle χ_1 undergoes rapid changes to $\chi_1 = 50°$ and remains stabilised in the *gauche*(−) rotameric state for periods of time sufficiently long to conclude that the *gauche*(−) rotamer is representative of the conformation of the side-chain of Glu62 when EF-3 is substituted by Mg^{2+} (note that spikes still occur all along the trajectory). As shown in Figure 4, the *gauche*(−) χ_1 rotamer is automatically accompanied by the $\chi_3 = -170°$ rotamer in the MD trajectory while the χ_2 angle remains constant at about −170° (not shown). Whether the *gauche*(−) rotamer about the χ_1 dihedral angle is the unique conformational state of the Glu62 side-chain, or whether there is a mixture of skewed *gauche*(+) and *gauche*(−) in equilibrium, remains an open question. It is to be noted that the variations of the dihedral angles are strongly correlated. One conformer (labelled I) of Glu62 would correspond to the following set of calculated dihedral angles: $\chi_1 = 50°$ (*gauche*(−)), $\chi_2 = -170°$ and $\chi_3 = -180°$, to be compared with the values observed with Glu101 in the EF-4 site occupied by Mg^{2+} (experimental values in 4pal: $\chi_1 = 62°$, $\chi_2 = -172°$ and $\chi_3 = -167°$) whereas a second conformer (labelled II) could be $\chi_1 = -30$ to $-40°$ (skewed *gauche* (+)), $\chi_2 = -160°$ and $\chi_3 = -90°$. No other conformer was predicted for Glu62 thus suggesting that the steric conditions provided by the protein at the level of Glu62 lead to a restricted number of conformations (two namely, if not a single one, upon Mg^{2+} co-ordination). NMR studies of the fully Mg-loaded form of pike 5.0 Pa have shown that both EF-3 and EF-4 sites behave symmetrically at the level of their χ_1 rotameric states for both Glu12 residues, i.e. Glu62 and Glu101. Moreover, based on two-dimensional ^1H NMR evidence, it was shown that Mg^{2+}-loaded EF-3 and EF-4 sites do not display the more stable *gauche*(+) rotamer which is found in their Ca^{2+}-loaded states (Blancuzzi *et al.*, 1993). Thus, our predictions are consistent with the NMR results in the sense that the simulated sites, EF-3 and EF-4, display the χ_1 *gauche*(−) rotamers for their Glu12 residues upon the alchemical transformation of Ca^{2+} into Mg^{2+}. As far as the conformational rearrangements of both side-chains of Glu62 and Glu101 upon Ca^{2+}/Mg^{2+}-exchange are concerned, as inferred from our calculations, we conclude that the two homologous residues which occupy the relative position 12 in the respective EF-hand loop sequences are likely to behave symmetrically. This was to be expected, given the approximate 2-fold symmetry that relates the EF-3 and EF-4 motifs within the EF-hand pair domain of parvalbumins (as initially described by Kretsinger & Nockolds, 1973). However, such a symmetry can only be approximate since, as shown by ^{113}Cd NMR, both sites EF-3 and EF-4 display distinct ^{113}Cd signals, as a consequence of

local differences between these sites (Drakenberg *et al.*, 1978).

On the other hand, the calculated free energies which in principle allow for the calculation of the K_{Ca}/K_{Mg} ratio for the affinities of the EF-4 site for Ca^{2+} and Mg^{2+} do not seem to be in agreement with presently available experimental evidence (note that, however, so far no values of K_{Ca} and K_{Mg} have been measured for the 4.10 isoform considered in the present work). Since our calculations only involved a subdomain of the protein centred around the cation bound to the EF-4 site, in which all atoms are left free to move whereas the remaining atoms are kept rigid or under defined constraints (see Materials and Methods), it is possible that free energy calculations which lead to a small negative $\Delta\Delta A(Ca^{2+} \rightarrow Mg^{2+})$ value are biased by such a truncation. Such a result is observed in the cases of the 4pal and 3pal structures (see Table 2). However, if the calculation is carried out starting from the 1pal crystal structure, the result is a large positive $\Delta\Delta A(Ca^{2+} \rightarrow Mg^{2+})$ value of nearly 6.5 kcal/mol which is consistent with all $\Delta\Delta A(Ca^{2+} \rightarrow Mg^{2+})$ values (3-5 kcal/mol) calculated in the case of the EF-3 site. Since in the case of 1pal, the third site is occupied by a monovalent cation whereas in 3pal and 4pal it is occupied by a divalent cation, namely Mg^{2+}, one can wonder whether there may be some long-range influence, direct or indirect, of the chemical nature of the cation bound to the third site on the respective affinities of the primary site EF-4 for Ca^{2+} and Mg^{2+}. As mentioned in the Introduction, such a third site has only been observed in the case of parvalbumins substituted by Asp61, as is the case of pike 4.10 where, based on X-ray crystallographic evidence, the third site was found to be located in the vicinity of the primary site EF-3. Thus, the putative effects of the third site on the binding capacity and selectivity of the primary EF-4 site for both divalent cations Ca^{2+} and Mg^{2+} are not easily rationalised, since the distance between both sites is quite significant (nearly 10 Å). However, the crystallisation in the presence of a large excess of Mg^{2+} of a defined molecular species in the case of pike 4.10 in which the EF-4 site is selectively substituted by Mg^{2+} and the EF-3 site is occupied by Ca^{2+} (crystal structure 4pal), suggests that under such conditions (full occupancy of the third site by Mg^{2+}), both primary sites may indeed differ markedly by their respective affinities for Ca^{2+} and Mg^{2+}. In future works, we will take advantage of the availability of the tertiary crystal structure of an alpha parvalbumin, determined at a resolution of 1.54 Å (Roquet *et al.*, 1992), with no third site, to confirm our results as well as our paradoxical hypothesis.

Note that Table 2 presents a set of alchemical Ca^{2+}/Mg^{2+} transformations within EF-3 and EF-4 sites of parvalbumin taken individually. Some of the simulated forms are expected to be highly represented in solution (and possibly under *in vivo* conditions), whereas others are much less abundant due to their relative thermodynamic stabilities. In their initial study of the binding of calcium ions by whiting parvalbumin by Trp fluorescence, Permyakov *et al.* (1980b) showed that Ca^{2+}-binding to the apo-protein can be described by the successive binding of two Ca^{2+} to the parvalbumin molecule with binding constants K_1 ca 5×10^8 M^{-1} and K_2 ca 6×10^6 M^{-1}. This conclusion is in contrast with an initial study (Benzonana *et al.*, 1972) of the binding of calcium to parvalbumins (major component pI 4.6 from hake muscle, *Merluccius merluccius*, and two major components, pI 4.88 and 4.50 from frog muscle, *Rana esculenta*) by the ^{45}Ca-Chelex partition method, in which it was concluded that these proteins have two high-affinity sites with similar affinities ($K_d = 0.1 \times 10^{-6}$ to 0.4×10^{-6} M; but measured in the presence of Mg^{2+}; see the Introduction). Based on high-resolution ^1H NMR spectroscopy, it is established that titration of the apoform PaCa0 (with both its sites EF-3 and EF-4 devoid of any divalent cation) of pike 5.0 parvalbumin with Ca^{2+} results in the occurrence of two one-calcium intermediate species, i.e. Pa0Ca and PaCa0, before the fully Ca-loaded species $PaCa_2$ is formed (Blancuzzi *et al.*, 1993). Titration with Mg^{2+} apparently results in the occurrence of a single one-magnesium intermediate species Pa(0,Mg) before formation of PaMgMg (Blancuzzi *et al.*, 1993). The possibility remains open that the intermediate state Pa(0,Mg) could be a mixture of both forms Pa0Mg and PaMg0 if the resolution achieved by NMR is not sufficient. The titration of PaMgMg with Ca^{2+} apparently involves a single intermediate species Pa(Ca,Mg) (Blancuzzi *et al*, 1993). The latter is likely to correspond to PaCaMg with EF-3 substituted by Ca^{2+} and EF-4 by Mg^{2+}, taking into account the occurrence of a single crystal form PaCaMg.Mg in the case of pike 4.10 parvalbumin (Declercq *et al.*, 1991). It thus appears that the filling of the two primary sites, EF-3 and EF-4 of parvalbumin, follows a complex pattern which depends on the initial state of the protein as well as on the nature of the cation itself. The simulated forms in Table 2, PaMgCa.Mg and $PaMgCa.NH_4$, even if they are thermodynamically unfavoured could thus occur under specific conditions in solution. However, in the present state of our study, it is likely that the interdependence between both sites (there is a hydrogen bond between the NH of Ile58 and the CO of Ile97, which links both loops; Kretsinger & Nockolds, 1973) at the structural and energetic levels is not well represented in our calculations. Since the alchemically transformed cation and all atoms away from the cation by more than 11 Å are kept fixed, the structural variations, therefore, do not include any variation of the intercationic distance EF-3/EF-4. This distance is slightly more than 11 Å in the crystal forms 1pal, 3pal and 4pal (Declercq *et al.*, 1991) being 11.79 and 11.94 Å for 1pal (PaCaCa.NH4) and 3pal (PaCaCa.Mg), respectively, and 11.48 Å for 4pal (PaCaMg.Mg). The simulated form PaCaMg.Mg starting from 3pal is, therefore, not totally realistic,

since the Ca(EF-3)-Mg(EF-4) distance remains identical with the Ca-Ca distance in 3pal. Similarly, the Mg-Mg distance in the simulated form PaMgMg.Mg is also unrealistic, since it is identical with the Ca-Mg distance in 4pal. As stated below, it is likely that the Mg-Mg distance in PaMgMg.Mg is less than the Ca-Mg distance (in PaCaMg.Mg). Indeed, the intercationic EF3/EF4 distance will certainly be a stringent test to validate future all-free-atoms calculations of parvalbumin. Note that, since the Mg^{2+} in the third site is only 5 Å away from Ca^{2+}(EF-3) in PaCaMg.Mg (4pal), it is free to move during the calculations, as are most of the atoms surrounding it. As expected, the alchemical transformation of 4pal into the simulated form PaMgMg.Mg shows that the distance Mg(EF-3)-Mg(third site) is shorter than the distance Ca(EF-3)-Mg(third site) in the initial form 4pal.

Other trends observed during our theoretical analysis are somewhat difficult to match with experimental data. Asp92 becomes a bidentate ligand after a small variation of the λ parameter when starting from the 4pal Mg^{2+}-loaded form. Even when Glu101 switches from a monodentate to a bidentate configuration, at $\lambda = 0.55$ (Figure 6(a), Asp92 remains a bidentate ligand up to $\lambda = 0.95$, so that the theoretically predicted structure of the Ca^{2+}-loaded EF-4 site corresponds with an octaco-ordinated Ca^{2+}, at variance with known features of EF-hand crystal structures, in which Ca^{2+} is always found to be heptaco-ordinated (Declercq *et al.*, 1988; Swain *et al.*, 1989). Although a co-ordination number of eight oxygen atoms around Ca^{2+} in the EF-4 site had been initially reported for the crystal structure of carp 4.25 parvalbumin (Kretsinger & Nockolds, 1973; Moews & Kretsinger, 1975), heptaco-ordination of Ca^{2+} found in the parvalbumin EF-4 site appears to be the rule, based on subsequent X-ray crystallographic analyses of several fully Ca^{2+}-loaded parvalbumins at high resolution (Declercq *etal.*, 1988, 1991, 1996; Roquet *et al.*, 1992; Swain *et al.*, 1989; McPhalen *et al.*, 1994). Moreover, we note an exchange of the oxygen atoms of Asp90($O^{\delta 1}$) and Asp92($O^{\delta 2}$) when crossing the borderline at $\lambda = 1$ (Figure 6(a)), so that during the backward transformation ($Ca^{2+} \rightarrow Mg^{2+}$) the octaco-ordination of the central cation down to $\lambda = 0.35$ is ensured through the participation of Asp90 as a bidentate ligand. It is interesting to consider here the case of the Mn^{2+}-loaded EF-4 site of parvalbumin, as available in the 2pal crystal structure of pike 4.10 parvalbumin with both sites EF-3 and EF-4 substituted by Mn^{2+}, as well as the third site (Declercq *et al.*, 1991). Mn^{2+} is a divalent cation with an ionic radius intermediate between the ionic radii of Ca^{2+} and Mg^{2+}. It is, therefore, expected that the λ variations during Ca^{2+}/Mg^{2+} exchange, as given in Figure 6(a), will lead, en passant, to the prediction of the geometrical features of the EF-4 site occupied by Mn^{2+}. However, no participation of Asp90 or Asp92 as bidentate ligands is observed at the level of the EF-4 site of the 2pal structure substituted by Mn^{2+} (Declercq *et al.*, 1991). Thus, it is likely that the octaco-ordination of Ca^{2+} observed in all our calculations is due to the inaccuracy of the description of Ca^{2+}-oxygen interactions through our potential energy function. As a matter of fact, the potential energy functions used by programs like CHARMM are not expected to perform well when the electrostatic interactions involved in the calculations are strong ones, as in the case of cation-carboxylate co-ordination, since in such programs all polarizability effects are only taken into account in an effective manner (Brooks *et al.*, 1983). In particular, the two oxygen atoms of the carboxylate group in glutamate residues are described as being equivalent, from the electrostatic point of view; both are considered to be partially charged, with $q = -0.57$. However, one expects that the electronic distribution in the carboxylate moiety will be significantly different when the carboxylate is involved in a direct interaction with Ca^{2+} in a monodendate or in a bidentate configuration. As a consequence, the monodendate configuration may prove more stable with respect to the bidentate one, than what it is in the present state of the description of cation-oxygen interactions in CHARMM. In order to test this hypothesis, new sets of parameters for describing cation-oxygen interactions are presently being developed. As a first step, a protocol allowing for parameters extraction from *ab initio* calculations on small enough systems has been designed (Periole *et al.*, 1997, 1998). The next step will be to include explicit polarizability in the classical description of the atoms. Note that one aspect of our present study is to show that meaningful results can be obtained using the present state of the potential energy function of CHARMM, without any explicit description of polarizability effects, even when quite polar binding sites are studied, as is the case of both EF-3 and EF-4 sites of Pa.

On the other hand, since atoms lying more than 11 Å away from the cation being alchemically transformed were held fixed during our simulations, the cation in the primary EF-4 site, therefore, corresponds to a fixed atom during the alchemical transformation of Ca^{2+} into Mg^{2+} within the EF-3 site, and this is likely to affect the simulated protein conformation. Indeed, it is known by X-ray crystallography with pike 4.10 parvalbumin, that the intercationic distance between sites EF-3 and EF-4 is dependent on the nature of the cation bound (Declercq *et al.*, 1991). The exchange of Ca^{2+} by Mg^{2+} in the EF-4 site thus results in a shortening of the cation-cation distance by 0.3-0.4 Å between sites EF-3 and EF-4. There is experimental evidence by ^1H NMR (pike 5.0 component) that the oxygen-Mg distances in the EF-3 site are reduced when Ca^{2+} is substituted by Mg^{2+}, thus accounting for the strong chemical shift variations of the hydroxyl proton of the invariant Ser55 that are induced (electric field effects)

upon changing the ionic radius of the bound cation (data not shown). The intercationic distance in Pa.MgMg.Mg (pike 4.10) is not presently known experimentally. Growing of crystals from the fully Mg-loaded form of pike 4.10 in solution (as assessed by ^{1}H NMR) only yielded the hybrid form Pa.CaMg.Mg (4pal; Declercq *et al.*, 1991). Although the fully Mg-loaded form of pike 5.0 parvalbumin, i.e. Pa.MgMg, with no third site in the presence of Glu61, has been characterised by two-dimensional ^{1}H NMR (Blancuzzi *et al.*, 1993; A. Cavé, unpublished results), the intercationic distance Mg^{2+}/Mg^{2+} is not presently available in pike 5.0 Pa.MgMg. Based on structural effects related to the Mg-co-ordination, one can speculate that the Mg^{2+}/Mg^{2+} distance in the fully Mg-loaded parvalbumin forms will be shorter by an additional 0.3-0.4 Å, so that the intercationic distance in this form will be about 11.1-11.2 Å: (i) all the oxygen-metal distances in EF-3 are shorter by 0.4 Å in comparison with Ca-co-ordination, as shown in our simulations; (ii) since both sites EF-3 and EF-4 are connected through hydrogen bonds (short anti-parallel β-strand), the shortening of the oxygen-metal distances in the EF-3 site upon substitution of Ca^{2+} by the smaller ion Mg^{2+} will bring the EF-3 and EF-4 sites closer (by 0.3-0.4 Å), assuming that the hydrogen bond pattern between both sites is not perturbed. However, in our simulations, the Mg^{2+} in the EF-4 site belongs to the class of fixed atoms (see Computational methods) during the alchemical transformation of Ca^{2+} into Mg^{2+} within the EF-3 site, starting from the crystal structure Pa.MgMg.Mg. Therefore, the final geometry of the simulated Pa.MgMg.Mg form does not include such subtle effects. This could be achieved only when FEP calculations on much larger systems, with two completely free EF-hand sites, are performed. Note that such calculations would be very lengthy.

The two Ca^{2+}/Mg^{2+}-binding sites of TnC in the C-terminal lobe of the protein molecule correspond with a pair of EF-hands with a high degree of homology at the level of their tertiary fold with the unique EF-hand pair domain of parvalbumin. Though it is assumed that the Mg-loaded forms are associated with the resting muscle whereas the Ca-loaded forms selectively interact with other muscle proteins in the contractile machinery and participate in muscle activation (Rüegg, 1989), and whereas a high-resolution crystal structure of a Ca-loaded form of TnC is already known, there are no experimental data concerning the tertiary structure of any Mg-loaded form of TnC. Starting from the 1.8 Å-resolution crystal structure of TnC with both its EF-3 and EF-4 sites substituted by Ca^{2+} (1top; Satyshur *et al.*, 1988), it appeared of interest to generate a Mg-loaded form of TnC, using the FEP approach which has been rather successful in predicting the geometry of both EF-hand sites of parvalbumin upon Ca^{2+}/Mg^{2+}-exchange. Again the essential role of the conformational flexibility of the glutamyl residue at the relative position 12 in the EF-hand sequence on Ca^{2+}/Mg^{2+} exchange is emphasised by our study of the transformation of the EF-3 site, initially loaded with Ca^{2+} in the crystal structure, into a Mg^{2+}-loaded site. In the case of the Ca^{2+}-Mg^{2+} binding EF-1 site of calmodulin (Tsai *et al.*, 1987), a similar conclusion is reached. A more detailed description of the simulated forms of TnC and CaM substituted by Mg^{2+} will be given elsewhere. Our results suggest that with respect to the Glu12 torsional angles, different situations may occur.

Conclusion

Our theoretical study supports the hypothesis that the invariant Glu residue at the relative position 12 in the cation-binding loops of the EF-hand proteins operates as an essential residue in Ca^{2+}/Mg^{2+} exchange through its ability to switch between different conformational states in such a way that the basic co-ordination requirements of the two physiologically relevant ions, Ca^{2+} and Mg^{2+}, can be met upon binding to the protein with no other major rearrangement of the global fold of the protein. Indeed, the positioning of the cation within the tertiary structure remains practically unperturbed in the tertiary structure while the Glu12 side-chain compensates for the differences in cation co-ordination. In the case of parvalbumin, both EF-3 and EF-4 sites require two conformationally distinct states of their Glu12 residues, which essentially differ by their χ_1 dihedral angles: *gauche*(+) and *gauche*(−) for the Ca^{2+} and Mg^{2+}-loaded states, respectively. It is possible that the *gauche*(+)/*gauche*(−) interconversion of Glu12 is not systematically associated with Ca^{2+}/Mg^{2+} exchange as suggested by our theoretical predictions with two other EF-hand proteins, troponin C and calmodulin, although in both cases Glu12 switches from a monodentate form (Mg^{2+}-loaded) to a bidentate one (Ca^{2+}-loaded). However, as far as this interconversion of the Glu12 side-chain is concerned, it is difficult to give a firm conclusion in the present state of our studies, since it proved difficult to predict. Indeed, in a set of studies starting from different Pa Ca^{2+}-loaded crystal structures (1pal, 3pal or 4pal), the experimentally known conformation of the Mg^{2+}-loaded form (in the EF-4 site) was successfully predicted, but only once (in the EF-3 site, starting from 4pal), and after a subsequent 100 ps MD simulation of the final state.

Finally, our theoretical prediction with an EF-hand protein containing Asp instead of Glu at position 12 (the sarcoplasmic binding protein) suggests that the substitution of the bismethylene side-chain of Glu by the monomethylene side-chain of Asp strongly reduces the conformational flexibility at position 12, so that Asp12 remains conformationally unperturbed (bidentate) during the simulation of Ca^{2+}/Mg^{2+} exchange. In this

case, other ligands in the EF-hand site are likely to participate in the differences of co-ordination with Ca^{2+} and Mg^{2+}.

Materials and Methods

High-resolution crystal structures

The Protein Data Bank codes of the studied structures are the following. For parvalbumin (Declercq *et al.*, 1991), 1pal; PaCaMg.NH_4, 3pal; PaCaCa.Mg, 4pal; PaCaMg.Mg. For troponin C (Satyshur *et al.*, 1988), 1top. For calmodulin (Chattopadhyaya *et al.*, 1992), 1cll. For the sarcoplasmic calcium-binding protein (Vijay-Kumar & Cook, 1992), 2scp.

Computational methods

Model

FEP requires an efficient sampling of the configurational space and, as a consequence, only protein sites can be studied with this method, using commonly available computer power. Therefore, systems studied were all built as follows: starting from the crystallographic structure, including crystallographic water, a 15 Å radius sphere of water molecules picked from an equilibrated cubic box was added around the cation, with all water molecules having their oxygen atom closer than 2.3 Å to a protein heavy (i.e. non-hydrogen) atom being removed. Then, all amino acid residues lying more than 15 Å away from the cation in the studied protein site were removed. Moreover, atoms lying more than 11 Å away from the cation were held fixed, as well as heavy atoms lying more than 9 Å away, and the cation itself. Thus, atoms were free to move in a 9 Å radius sphere, surrounded by a soft boundary in which water molecules, for instance, were only free to rotate.

Force field

The CHARMM-22 force field with ''extended'' CH_3, CH_2, and CH atoms (Brooks *et al.*, 1983) was used for the calculation of energies and forces in the system, the water molecules being modelled with a three-point-charge model, namely the TIP3P model (Jorgensen *et al.*, 1983), which had been specifically developed for mixed protein/water system studies; the corresponding parameters are given, for instance, by Alary *et al.* (1993). During the molecular dynamics runs, a 14 Å cutoff was used for coulombic and Lennard-Jones interactions, together with a SHIFT truncation procedure, which was designed in order to smooth the interaction function near the cutoff value (Brooks *et al.*, 1983). The dielectric constant was set to unity.

Parameters used to describe the cation-oxygen Lennard-Jones interaction are those determined by J. Åqvist. With this parameter set, radial distribution functions of water oxygen atoms around each cation are very well reproduced in MD simulations, as well as their absolute hydration free energies, in FEP calculations (Åqvist, 1990). Note that the parameters for cation-protein oxygen Lennard-Jones interactions were deduced from Åqvist's values using Berthelot-Lorentz rules, as they are implemented in CHARMM, taking care of the fact that a different set of rules is implemented in the program used in the original study (Åqvist, 1994). It was checked that Åqvist's results for divalent cations in a water environment can be reproduced using CHARMM, such a parameter set, and our 15 Å radius sphere with-a-soft-boundary model (data not shown).

Minimisation and molecular dynamics simulations

In order to release the potential energy excess due to short interatomic distances which may appear as a result of the model-building process, or as a consequence of the fact that the crystallographic structure is spatially averaged over all crystal cells, 500 minimisation steps were performed, with the conjugate gradient algorithm available in CHARMM (harmonic constraints were imposed on protein atom positions during this process, with $k = 50$ kcal mol^{-1} Å^{-2}).

In order to integrate the equations of atomic motion, the Verlet integration algorithm was used (Verlet, 1967). Since protein and water bond lengths were constrained to their equilibrium values, with the SHAKE algorithm (Ryckaert *et al.*, 1977), a timestep of 2 fs was chosen (Van Gunsteren & Karplus, 1982).

During the first 3 ps, the system was thermalized by progressively modifying the atomic velocities, in order to reach an averaged 300 K temperature. Then, during 15 ps, the system was equilibrated, that is, the atomic velocities were periodically checked (every 500 steps), and reassigned according to an overall scaling, when the averaged temperature was found to be outside a 5 K window around the expected 300 K temperature.

Free energy difference calculations

With the free energy perturbation method, differences between the binding free energies of two ligands (labelled A and B) of a given protein can be computed, by progressively transforming one ligand into the other in a water environment on the one hand, and within a protein site on the other hand. All along such ''computer alchemical'' transformations, the environment of the ligand in water or in the protein is supposed to change in a quasi-continuous way, so that accurate samples of the part of the configurational space in which there are some differences in the environment of the two ligands can be obtained.

Such transformations are achieved by using a hybrid potential energy function:

$$V(r^N, \lambda) = (1 - \lambda)V_A(r^N) + \lambda V_B(r^N)$$

where λ is a coupling parameter varying from 0 to 1, all along the calculation, and where $V_A(r^N)$ and $V_B(r^N)$ are, respectively, the potential energies of interaction of ligand A and B with their environment, for a given set of atomic coordinates, r^N. The free energy difference between states A and B, i.e. ΔA_{AB}, can then be obtained from (Zwanzig, 1954; Bennett, 1975):

$$\Delta A_{AB} = -k_B T \sum_i^{m_s} \ln\langle e^{-V(r^N,\lambda_i+\Delta\lambda)-V(r^N,\lambda_i)/k_B T}\rangle_{\lambda_i}$$

where k_B is the Boltzmann constant, T the absolute temperature, and where the brackets indicate that an ensemble average has to be computed for each of the λ_i values. Note that there is no approximation involved in the above formula.

From a practical point of view, starting from the end of a 10 ps equilibration period during which $\lambda = 0.05$, a series of ten MD simulations is performed. In each simulation, i.e. for a given λ_i value, the system is first equili-

brated over a 5 ps time span, and then, from the following 10 ps trajectory, a sample of 500 configurations is picked, from which the ensemble average involved in the above formula is calculated, both for $\Delta\lambda = -0.05$ and $\Delta\lambda = +0.05$. Then, λ is increased by $\Delta\lambda = 0.1$, the last point of the previous simulation being the first point of the next one, etc. Finally, starting from the $\lambda = 0.95$ value, a backward transformation is performed, so as to obtain a measure of the quality of the calculation (the free energy difference along the round-trip path $\lambda = 0 \rightarrow \lambda = 1 \rightarrow \lambda = 0$ should be zero, if a perfect sampling has been obtained, and if no systematic drift has occurred during the calculation).

Acknowledgements

This work was supported by the Centre National de la Recherche Scientifique (CNRS, Paris, France; grant PICS n°141; GDR 1150). We thank Professor Jean Durup for his interest and for fruitful discussions, as well as one referee for helpful suggestions. Grants of computer time c96059 and c97059, from the C.N.U.S.C. (Montpellier, France) are acknowledged. J.P. was an Adjunct Professor at the Burnham Institute (1993-1998).

References

Alary, F., Durup, J. & Sanejouand, Y.-H. (1993). Molecular dynamics study of the hydration structure of an antigen-antibody complex. *J. Phys. Chem.* **97**, 13864-13876.

Allouche, D. (1997). Etude du comportement de calciprotéines à mains EF en présence de calcium et de magnésium à partir de trajectoires de dynamique moléculaire et de calculs de différences d'énergie libre. PhD thesis, Université Paul Sabatier, Toulouse, France.

Åqvist, J. (1990). Ion-water interaction potentials derived from free energy perturbation simulations. *J. Phys. Chem.* **94**, 8021-8024.

Åqvist, J. (1994). Comments on ''transferability of ion models''. *J. Phys. Chem.* **98**, 8253-8255.

Bennet, W. (1975). Mass tensor molecular dynamics. *J. Comput. Phys.* **19**, 267-279.

Benzonana, G., Capony, J.-P. & Pechère, J.-F. (1972). The binding of calcium to muscular parvalbumins. *Biochim. Biophys. Acta,* **278**, 110-116.

Berchtold, M. W., Celio, M. R. & Heizmann, C. W. (1985). Parvalbumin in human brain. *J. Neurochem.* **45**, 235-240.

Blancuzzi, Y. (1993). Etude par RMN protonique de l'échange Ca^{2+}/Mg^{2+} en série calciprotéique (parvalbumine de brochet pI 5,0). PhD thesis, Université Montpellier II, France.

Blancuzzi, Y., Padilla, A., Parello, J. & Cavé, A. (1993). Symmetrical rearrangement of the cation-binding sites of parvalbumin upon Ca^{2+}/Mg^{2+} exchange. A study by ^{1}H 2D NMR. *Biochemistry,* **32**, 1302-1309.

Blümcke, I., Hof, P. R., Morrison, J. H. & Celio, M. R. (1990). Distribution of parvalbumin in the visual cortex of old world monkeys and humans. *J. Comp. Neurol.* **301**, 417-432.

Breen, P. J., Johnson, K. A. & Horrocks, W. D. (1985). Stopped-flow kinetic studies of metal ion dissociation or exchange in a tryptophan-containing parvalbumin. *Biochemistry,* **24**, 4997-5004.

Brooks, B. R., Bruccoleri, R. E., Olafson, B. D., States, D. J., Swaminathan, S. & Karplus, M. (1983). CHARMM: A program for macromolecular energy, minimisation, and dynamics calculations. *J. Comp. Chem.* **4**, 187-217.

Cavé, A., Daurès, M. F., Parello, J., Saint-Yves, A. & Sempéré, R. (1979). NMR studies of primary and secondary sites of parvalbumin using the two paramagnetic probes Gd(III) and Mn(II). *Biochimie,* **61**, 755-765.

Cavé, A., Parello, J. & Saint-Yves, A. (1981). Ion-binding by muscular parvalbumins of the alpha phylogenetic series: A proton relaxation enhancement study with pike 5.0 parvalbumin. *Biochimie,* **63**, 457-461.

Cavé, A., Saint-Yves, A., Parello, J., Swärd, M., Thulin, E. & Lindman, B. (1982). NMR studies on parvalbumin phylogeny and ionic interactions. *Mol. Cell. Biochem.* **44**, 161-172.

Celio, M. R. (1986). Parvalbumin in most γ-aminobutyric acid-containing neurons of the rat cerebral cortex. *Science,* **231**, 995-996.

Chattopadhyaya, R., Meador, W. E., Means, A. R. & Quiocho, F. A. (1992). Calmodulin structure refined at 1.7 Å resolution. *J. Mol. Biol.* **228**, 1177-1192.

Cox, J. A., Wnuk, W. & Stein, A. (1977). In *Calcium-binding Proteins and Calcium Function* (Wasserman, H. *et al.*, ed.), pp. 266-269, Elsevier North Holland, New York.

Declercq, J. P., Tinant, B., Parello, J., Etienne, G. & Huber, R. (1988). Crystal structure determination and refinement of pike 4.10 parvalbumin (minor component from *Esoxlucius*). *J. Mol. Biol.* **202**, 349-353.

Declercq, J. P., Tinant, B., Parello, J. & Rambaud, J. (1991). Ionic interactions of parvalbumin. Crystal structure of pike 4.10 parvalbumin in four different ionic environments. *J. Mol. Biol.* **220**, 1017-1039.

Declercq, J. P., Tinant, B. & Parello, J. (1996). X-ray structure of a new crystal form of pike-4.10 beta-parvalbumin. *Acta Crystallog. sect. D,* **52**, 165-169.

Drakenberg, T., Lindman, B., Cavé, A. & Parello, J. (1978). Non-equivalence of the CD and EF sites of muscular parvalbumins. A ^{113}Cd NMR study. *FEBS Letters,* **92**, 346-350.

Drakenberg, T., Swärd, M., Cavé, A. & Parello, J. (1985). Metal-ion binding to parvalbumin. A ^{113}Cd-n.m.r. study of the binding of different lanthanide ions. *Biochem. J.* **227**, 711-717.

Falke, J. J., Drake, S. K., Hazard, A. L. & Peersen, O. B. (1994). Molecular tuning of ion binding to calcium signaling proteins. *Quart. Rev. Biophys.* **27**, 219-290.

Gillis, J. M., Thomason, D., Lefèvre, J. & Kretsinger, R. H. (1982). Parvalbumin and muscle relaxation: a computer simulation study. *J. Muscle Res. Cell Motil.* **3**, 377-398.

Gomer, R. & Tryson, G. (1977). An experimental determination of absolute half-cell emf's and single ion free energies of solvation. *J. Chem. Phys.* **66**, 4413-4424.

Haiech, J., Derancourt, J., Pechère, J. F. & Demaille, J. G. (1979). Magnesium and calcium binding to parvalbumins: evidence for their difference between parvalbumins and an explanation of their relaxing function. *Biochemistry,* **18**, 2752-2758.

Hartig, W., Bruckner, G., Brauer, K., Seeger, G. & Bigl, V. (1996). Triple immunofluorescence labelling of

parvalbumin, calbindin-D28k and calretinin in rat and monkey brain. *J. Neurosci. Methods,* **67**, 89-95.

Hou, T. T., Johnson, J. D. & Rall, J. A. (1992). Effect of temperature on relaxation rate and Ca^{2+}, Mg^{2+} dissociation rates from parvalbumin of frog muscles. *J. Physiol.* **449**, 399-410.

Jorgensen, W. L., Chandrasekhar, J., Madura, J. D., Impey, R. W. & Klein, M. L. (1983). Comparison of simple potential functions for simulating liquid water. *J. Chem. Phys.* **79**, 926-935.

Kaufman-Katz, A., Glusker, J. P., Beeb, S. A. & Bock, C. W. (1996). Calcium ion coordination: a comparison with that of beryllium, magnesium, and zinc. *J. Am. Chem. Soc.* **118**, 5752-5763.

Kawasaki, H. & Kretsinger, R. H. (1994). Calcium-binding proteins 1: EF-hands. *Protein Profile,* **1**, 343-517.

Kollman, P. (1993). Free energy calculations: applications to chemical and biochemical phenomena. *Chem. Rev.* **93**, 2395-2417.

Kraulis, P. (1991). Molscript: a program to produce both detailed and schematic plots of protein structures. *J. Appl. Crystallog.* **24**, 946-950.

Kretsinger, R. H. & Nockolds, C. E. (1973). Carp muscle calcium-binding protein. II. Structure determination and general description. *J. Biol. Chem.* **248**, 3313-3326.

Marcus, Y. (1994). A simple empirical-model describing the thermodynamics of hydration of ions of widely varying charges, sizes and shapes. *Biophys. Chem.* **51**, 111-127.

McPhalen, C. A., Sielecki, A. R., Santarsiero, B. D. & James, M. N. G. (1994). Refined crystal structure of rat parvalbumin, a mammalian alpha-lineage parvalbumin, at 2 Å resolution. *J. Mol. Biol.* **235**, 718-732.

Moews, P. C. & Kretsinger, R. H. (1975). Refinement of the structure of carp muscle calcium-binding parvalbumin by model building and difference fourier analysis. *J. Mol. Biol.* **91**, 201-228.

Nara, M., Tasumi, M., Tanokura, M., Hiraoki, T., Yazawa, M. & Tsutsumi, A. (1994). Infrared studies of interaction between metal ions and Ca(2+)-binding proteins. Marker bands for identifying the types of coordination of the side-chain COO- groups to metal ions in pike parvalbumin (pI = 4.10). *FEBS Letters,* **349**, **(1)**, 84-88.

Ohtaki, H. & Radnai, T. (1993). Structure and dynamics of hydrated ions. *Chem. Rev.* **93**, 157-1204.

Pechère, J. F., Derancourt, J. & Haiech, J. (1977). The participation of parvalbumins in the activation-relaxation cycle of vertebrate fast skeletal-muscle. *FEBS Letters,* **75**, 111-114.

Periole, X., Allouche, D., Daudey, J. P. & Sanejouand, Y. H. (1997). Simple two-body cation-water interaction potentials derived from ab initio calculations. Comparison to results obtained with an empirical approach. *J. Phys. Chem. B,* **101**, 5018-5025.

Periole, X., Allouche, D., Ramirez-Solis, A., Ortega-Blake, I., Daudey, J. P. & Sanejouand, Y. H. (1998). New effective potentials extraction method for the interaction between cations and water. *J. Phys. Chem. B,* **102**, 8579-8587.

Permyakov, Y. A., Yarmolenko, V. V., Yemel'Yanenko, V. I., Burstein, E. A., Closset, J. & Gerday, C. (1980a). Fluorescence studies of the calcium-binding to whiting (*gadus-merlangus*) parvalbumin. *Eur. J. Biochem.* **109**, 307-315.

Permyakov, Y. A., Yarmolenko, V. V., Yemel'Yanenko, V. I., Burstein, E. A., Gerday, C. H. & Closset, J. (1980b). Study of the binding of calcium ions by whiting parvalbumin based on change in the parameters of the intrinsic fluorescence of protein. *Biophysics,* **25**, 430-436.

Pfyffer, G. E., Faivre-Bauman, A., Tixier-Vidal, A., Norman, A. W. & Heizmann, C. W. (1987). Developmental and functional studies of parvalbumin and calbindin D28k in hypothalamic neurons grown in serum-free medium. *J. Neurochem.* **49**, 442-451.

Potter, J. D. & Gergely, J. (1975). The Calcium and Magnesium Binding Sites on Troponin and Their Role in the Regulation of Myofibrillar Adenosine Triphosphate. *J. Biol. Chem.* **250**, 4628-4633.

Rhee, M.-J., Sudnick, D. R., Arkle, V. K. & Horrocks, W. DeW., Jr. (1981). Lanthanide ion luminescence probes. Characterization of metal ion binding sites and intermetal energy transfer distance measurements in calcium-binding proteins. 1. Parvalbumin. *Biochemistry,* **20**, 3328-3334.

Robertson, S. P., Johnson, J. D. & Potter, J. D. (1981). The time-course of Ca^{2+} exchange with calmodulin, troponin, parvalbumin, and myosin in response to transient increases in Ca^{2+}. *Biophys. J.* **34**, 559-569.

Roquet, F., Declercq, J. P., Tinant, B., Rambaud, J. & Parello, J. (1992). Crystal structure of the unique parvalbumin component from muscle of leopard shark (*Triakissemifasciata*). The first X-ray study of an α-parvalbumin. *J. Mol. Biol.* **223**, 705-720.

Rüegg, J. C. (1989). *Calcium in Muscle Activation*, Springer Verlag, Berlin.

Ryckaert, J. P., Ciccotti, G. & Berendsen, H. J. C. (1977). Numerical integration of the cartesian equations of motion of a system with constraints: molecular dynamics of n-alkanes. *J. Comput. Phys.* **23**, 327-341.

Satyshur, K. A., Rao, S. T., Pyzalska, D., Drendel, W., Greaser, M. & Sundaralingam, M. (1988). Refined structure of chicken skeletal muscle troponin C in the two-calcium state at 2 Å resolution. *J. Biol. Chem.* **263**, 16620-16628.

Strynadka, N. C. J. & James, M. N. G. (1989). Crystal Structures of the helix-loop-helix calcium-binding proteins. *Annu. Rev. Biochem.* **58**, 951-998.

Swain, A. L., Kretsinger, R. H. & Amma, E. L. (1989). Restrained least squares refinement of native (calcium) and cadmium-substituted carp parvalbumin using X-ray crystallographic data at 1.6 Å resolution. *J. Biol. Chem.* **264**, 1628-1647.

Tsai, M. D., Drakenberg, T., Thulin, E. & Forsén, S. (1987). Is the binding of magnesium significant? An investigation by magnesium-25 nuclear magnetic resonance. *Biochemistry,* **26**, 3635-3643.

Van Gunsteren, W. F. & Karplus, M. (1982). Effect of constraints on the dynamics of macromolecules. *Macromolecules,* **15**, 1528-1543.

Verlet, L. (1967). Computer experiments on classical fluids. I. Thermodynamic properties of Lennard-Jones molecules. *Phys. Rev.* **159**, 98-103.

Vijay-Kumar, S. & Cook, W. J. (1992). Structure of a sarcoplasmic calcium-binding protein from *Nereis diversicolor* refined at 2.0 Å resolution. *J. Mol. Biol.* **224**, 413-426.

White, H. D. (1988). Kinetic mechanism of calcium binding to whiting parvalbumin. *Biochemistry,* **27**, 3357-3365.

Wnuk, W., Cox, J. A. & Stein, E. A. (1982). Parvalbumins and other soluble high-affinity calcium-binding proteins from muscles. In *Calcium and Cell Function*. (Cheung, W. Y., ed.), vol. 2, pp. 243-278, Academic Press, New York.

Zwanzig, R. W. (1954). High-temperature equation of state by a perturbation method. I. Nonpolar gases. *J. Chem. Phys.* **22**, 1420-1426.

Edited by R. Huber

(Received 26 May 1998; received in revised form 5 October 1998; accepted 12 October 1998)